Discover Oncology

Research

Revealing the prognostic potential of natural killer cell-related genes in hepatocellular carcinoma: the key role of NRAS

Ruixi Li[1] · Guangquan Zhang[1] · Qiang Tao[1] · Ziyun Wu[2] · Xiaoping Liu[2] · Rongrong Wang[2] · Lei Liu[3] · Yiran Niu[2] · Kaile Du[2] · Runpeng Wu[2] · Fei Du[1] · Xiyan Zheng[1] · Yingliang Li[4] · Xianjie Shi[1]

Received: 9 August 2024 / Accepted: 21 March 2025
Published online: 18 May 2025

Abstract
Hepatocellular carcinoma (HCC) is a common malignancy associated with high morbidity and mortality rates worldwide. To improve the prognosis of HCC, early diagnosis is crucial. However, to date, little is known about the role of natural killer cell-related genes (NKCRGs) in predicting the prognosis of hepatocellular carcinoma patients. In this study, we identified 24 differentially expressed NKCRGs in HCC specimens from the TCGA dataset, including 22 upregulated genes and 2 downregulated genes. Functional enrichment analysis revealed that these genes were mainly involved in immune response pathways and various cancer-related pathways. Univariate analysis identified 21 prognostic NKCRGs, with eight genes (PAK1, MAP2K2, MAPK3, PLCG1, SHC1, HRAS, NRAS, and MICB) confirmed to be involved in HCC prognosis through Venn diagram analysis. A prognostic model was developed using LASSO-Cox regression, incorporating four genes (MAP2K2, SHC1, HRAS, and NRAS). The model's risk score was significantly associated with overall survival (OS) in both the TCGA and ICGC cohorts. Patients with high-risk scores had poorer OS, as demonstrated by Kaplan–Meier curves and ROC analyses. The risk score was not significantly correlated with gender or age but was higher in patients with advanced tumor grades and stages. Immune status analysis using ssGSEA showed higher enrichment scores for various immune cells and pathways in the high-risk group. Additionally, the risk score was positively correlated with the immune score, indicating its potential role in tumor microenvironment modulation. Expression analysis revealed that HRAS, SHC1, MAP2K2, and NRAS were upregulated in HCC tissues, with higher expressions of HRAS, MAP2K2, and NRAS associated with shorter OS. Knockdown experiments confirmed that silencing NRAS suppressed the proliferation of HCC cells, highlighting its potential as a therapeutic target. Overall, our findings suggest that the identified NKCRGs, particularly NRAS, play crucial roles in HCC progression and could serve as valuable prognostic markers and therapeutic targets.

Keywords Hepatocellular carcinoma · Natural killer cell-related genes · Prognostic markers · Tumor microenvironment · Drug sensitivity · NRAS

Ruixi Li, Guangquan Zhang, Qiang Tao have contributed equally.

✉ Yingliang Li, liyingliang1977@163.com; ✉ Xianjie Shi, shixj7@mail.sysu.edu.cn | [1]Department of Hepatobiliary and Pancreatic Surgery, The Eighth Affiliated Hospital, Sun Yat-Sen University, Shenzhen 518033, China. [2]The First Clinical Medical College of Nanchang University, Nanchang 330031, China. [3]Department of Clinical Pharmacy, The Eighth Affiliated Hospital, Sun Yat-Sen University, Shenzhen 518033, China. [4]Department of Breast Disease Center, The First Affiliated Hospital, Jiangxi Medical College, Nanchang University, Nanchang 330006, China.

1 Introduction

Liver cancer represents one of the most fatal malignancies, with cancer-induced fatalities nearing 30,000 annually [1]. Hepatocellular carcinoma (HCC) constitutes the predominant form of liver cancer, comprising approximately 70–85% of all instances [2]. HCC is highly prevalent in East Asia and sub-Saharan Africa. This high incidence is typically associated with the high prevalence of infections caused by hepatitis B virus (HBV) and hepatitis C virus (HCV) [3, 4]. In contrast, the incidence of HCC in Western countries is relatively lower, although it has been rising in recent years due to the increase in non-alcoholic fatty liver disease (NAFLD) and liver cirrhosis. HCC is more common in males, with an incidence approximately 2–3 times higher than in females. This gender disparity may be related to factors such as male hormones and the modes of transmission of HBV and HCV infections [5, 6]. Despite significant advances in early diagnosis and interdisciplinary cancer care, the long-term prognosis remains poor. Clinical outcomes could be improved by utilizing a reliable predictive model that accurately identifies patients at the highest risk for recurrence and metastasis [7, 8]. Conventional models for predicting HCC prognosis rely on a range of biomarkers, including clinical tumor-node-metastasis (TNM) staging and evaluation of vascular invasion. However, the prediction accuracy of these traditional models remains insufficient due to the high variability in HCC. When developing new predictive approaches, it is crucial to carefully consider molecular markers.

The tumor microenvironment (TME) encompasses the various non-cancerous cells, extracellular matrix (ECM), along with blood vessels, immune cells, and signaling molecules, which plays a critical role in the environment surrounding tumor cells [9]. This complex environment significantly influences tumor development, progression, and response to treatment. Non-cancerous cells, such as cancer-associated fibroblasts (CAFs), endothelial cells, and various immune cells, play crucial roles [10, 11]. CAFs secrete factors that can enhance tumor growth and invasion, while endothelial cells are integral to the abnormal blood vessel formation within tumors. Immune cells can both suppress and promote tumor growth depending on their state and interactions within the TME [12, 13]. The ECM provides structural support and participates in signaling that affects tumor cell behavior. Tumor blood vessels are often irregular and poorly structured, contributing to uneven blood flow and hypoxia within the tumor. The immune microenvironment often exhibits immunosuppressive characteristics, such as the recruitment of regulatory T cells and the production of suppressive cytokines, which help tumors evade immune detection. Chronic inflammation within the TME can also fuel tumor development [14, 15]. Natural Killer (NK) cells are crucial components of the innate immune system, responsible for identifying and eliminating infected or tumor cells. They play a significant role in immune surveillance by recognizing and destroying cells that exhibit abnormal surface markers or reduced MHC-I expression [16, 17]. NK cells are capable of targeting and killing cancer cells and virus-infected cells without the need for prior sensitization [18, 19]. They exert their effects through various mechanisms, including the release of cytotoxic granules such as perforin and granzymes, as well as the secretion of cytokines like interferon-γ and tumor necrosis factor-α, which enhance immune responses. NK cells are equipped with activating receptors that boost their activity and inhibitory receptors that prevent damage to normal cells by interacting with MHC-I molecules. Their development takes place in the bone marrow, and their activation can be influenced by factors such as infection, tumor transformation, or inflammation [20–22]. In clinical settings, NK cells are being explored for cancer immunotherapy and organ transplantation, highlighting their potential to enhance therapeutic outcomes and improve immune responses. Furthermore, NK cells are better than T cells at boosting responses to radiation and chemotherapy, numerous studies on antitumor immunity have shown that NK cells and T cells work together to regulate tumor advancement [23, 24]. In addition, prior research has shown that a higher concentration of tumor-infiltrating NK cells in certain types of cancer is significantly linked to improved clinical results. Several published studies have proposed molecular characteristics of NK cells in infectious diseases and malignant tumors, Considering the essential functions of tumor-infiltrating NK cells in the context of anti-tumor immunity. However, the relationship between NK cells and the prognosis of patients with HCC remains unclear.

This research aimed to create an innovative assessment framework for HCC that demonstrates significant promise in forecasting patient prognosis and treatment outcomes. The research involved analyzing RNA-seq expression profiles of HCC utilizing datasets from TCGA and the ICGC to identify independent prognostic genes associated with NK cells. This analysis established a prognostic signature for HCC based on four NK cell-related genes. to functional experiments were conducted to validate the clinical relevance of these genes and investigate their roles in HCC progression. These experiments aimed to elucidate how these NK cell-related genes might influence tumor growth, metastasis, or response to treatment. The findings suggest that NK cell-related genes play a significant role in HCC

and that their expression profiles could be used to develop a prognostic tool for better patient management. Additionally, based on existing literature and the study's results, integrating NK cell therapy with conventional treatments such as chemotherapy, targeted therapy, or immunotherapy may emerge as a promising strategy for improving treatment outcomes in HCC patients.

2 Methods

2.1 Data collection (TCGA-LIHC Cohort and ICGC (LIRI-JP) Cohort

The data used in this study were obtained from the TCGA database, which includes 370 HCC samples and 50 normal control samples. These samples were sourced from the TCGA-LIHC project, with the HCC samples being tumor tissues from patients diagnosed with HCC, and the normal control samples being paired normal liver tissues from the same patients, ensuring consistency in sample source and processing. During data extraction, we followed the TCGA database's standard selection process, excluding any samples with missing or incomplete data. Additionally, repeated samples were checked, ensuring that only one sample per patient was included in the analysis to guarantee the accuracy and reproducibility of the data. The ICGA website was used to get clinical information and RNA sequencing data for an additional 231 tumor samples. Following their separate data access policies and publication criteria, both the ICGC and TCGA made their data publicly available. A plethora of data on different types of cancer has been made available by TCGA, a thorough and coordinated effort to speed up our knowledge of the molecular basis of cancer by applying genome analysis methods. In a similar vein, fifty different tumor types and subtypes will be thoroughly characterized by ICGC in terms of genomic, transcriptomic, and epigenomic changes. A plethora of cancer research projects are made possible by these publicly available datasets, which include omics data, DNA methylation, whole genome sequencing, and RNA sequencing. Cancer research has progressed and patients have improved diagnostic and treatment choices because of the ICGA database, which provides researchers with access to a large volume of high-quality genomic data. Both the TCGA and ICGC data sets were made publicly available in accordance with their respective data access policies and publishing requirements. For the preprocessing of RNA data, we downloaded raw RNA sequencing data from the TCGA and ICGC databases and performed initial quality control to remove low-quality samples (e.g., samples with low gene expression or batch effects). All data were standardized to eliminate batch effects and technical differences between samples. We used the RPKM (Reads Per Kilobase of transcript per Million mapped reads) method for normalization to ensure data consistency and comparability. To improve the accuracy of the analysis, we filtered out genes with low expression across all samples and retained only those genes with detectable expression levels in a subset of samples. Next, the Molecular Signatures database yielded results for natural killer cell-related genes (NKCRGs).

2.2 Development of a prognostic NKCRGs signature

Our initial step in identifying DEGs in the TCGA cohort was to use the "limma" R tool to compare tumor and non-tumor tissues. To ensure that the selected genes exhibited significant expression differences, the filtration criteria were adjusted, setting a fold change (FC) greater than 2 and a false discovery rate (FDR) below 0.05. We next used these DEGs to find NKCRGs (natural killer cell-related genes) that had prognostic significance by running a univariate Cox regression. We employed the "glmnet" R package to conduct LASSO-penalized Cox regression analysis, thereby constructing a robust prognostic model. To prevent overfitting, this approach adds a penalty term to account for variables being selected and coefficients being shrunk. To make sure the model can be applied to different situations, A ten-fold cross-validation technique was employed to determine the optimal penalty parameter (lambda).. We computed risk scores for every patient using the expression levels and regression coefficients of every NKCRG. To conduct additional comparisons and analyses, patients were then divided into low-risk and high-risk groups based on their median risk scores. We employed t-Distributed Stochastic Neighbor Embedding (t-SNE) alongside principal component analysis (PCA) for our analysis to examine whether there were any variations in gene expression distribution between the low-risk and high-risk groups. These studies were useful for visualizing the shared characteristics and expression patterns among the various groups. We employed survival analysis to examine the overall survivals rates between the high-risk and low-risk cohorts to determine the effectiveness of the prognostic model. Cox regression analysis further confirmed the 4-gene signature's prognostic utility, and its predictive value was assessed using time-dependent ROC curve analysis.

2.3 Tumor microenvironment and immune response analysis

The levels of immune and stromal cell infiltration in various tumor tissues were investigated in this study. The stromal and immune scores were computed to initiate the evaluation of the level of these cell infiltrations. Using Spearman correlation analysis, we looked at how the risk score was related to the immunological and stromal scores. We also performed a 2-way ANOVA to examine the differences in immune cell infiltration across risk scores, as this might provide light on the nature of the association between the risk score and other forms of immune infiltration. In order to measure the stem cell-like properties of cancers, researchers derived tumor stem cell features using the transcriptomic and epigenetic data of TCGA tumor samples. Afterwards, the Spearman correlation analysis was used to assess the link between tumor stemness and risk score. The correlations between the risk score, stromal cell and immune cell infiltration, and stem cell traits were clarified by these investigations.

2.4 Chemotherapy sensitivity analysis

The CellMiner platform was used to retrieve data from the NCI-60 database, which includes 60 distinct cancer cell lines from nine different tumor types (https://discover.nci.nih.gov/cellminer). Using Pearson correlation analysis, we examined the relationships between gene expression levels and drug sensitivity. We focused on 263 FDA-approved drugs or those in clinical trials, investigating whether there was a correlation between the expression levels of prognostic genes and drug efficacy, as measured by metrics such as IC50. Our aim was to identify potential correlations between gene expression and drug susceptibility, enabling personalized treatment strategies based on an individual patient's genetic profile. The data were preprocessed and normalized, with several testing modifications applied to ensure robustness. In addition to interpreting the results in the context of established biological pathways and drug mechanisms, we also considered the possibility of validating our findings through other datasets or experimental confirmation.

2.5 Functional enrichment analysis

Enrichment assays were carried out by the use of the "clusterProfiler" R package to analyze the functional annotations of Natural Killer (NK) cell-related genes. Gene Ontology (GO) analysis categorized these genes into three main domains: Molecular Functions (MF), Biological Processes (BP), and Cellular Components (CC). GO analysis describes the biochemical activities (MF), biological objectives (BP), and cellular locations (CC) of gene products. Additionally, the KEGG (Kyoto Encyclopedia of Genes and Genomes) pathway analysis was utilized to investigate the functions of these genes within particular biochemical pathways and networks. integrating information on chemical, genetic, and systemic functions. Both GO and KEGG analyses were conducted with a significance threshold set at $P < 0.05$ to identify significantly enriched terms and pathways. During data preparation, gene identifiers were matched with those in the GO and KEGG databases, and multiple testing corrections, such as the Benjamini–Hochberg procedure, were applied to adjust for false discovery rates. The results were interpreted within the biological context of immune-related processes, providing deeper insights into the functional roles of NK cell-related genes.

2.6 Cell culture and cell transfection

Procured from the Cell Bank at the Chinese Academy of Sciences in Shanghai, China., the following human HCC cell lines were used: SK-Hep-1, HUH7, MHCC97-H, HCCLM3, and the immortalized hepatic cell line L02. These cells were refined in Dulbecco's Changed Hawk Medium (DMEM, Hyclone, Logan, Utah, USA) with 10% fetal cow-like serum (FBS, Gibco, Excellent Island, NY, USA) at 37 °C in a humidified hatchery with 5% CO2. Before transfection, cells were grown to 70–80% confluence in 6-well or 12-well plates. To transfect the cells, researchers utilized Lipofectamine 2000 reagent from Invitrogen in California, USA. The cells were then transfected with siRNAs si-NRAS and si-NC, both of which were manufactured by GenePharma in Shanghai, China. Prior to adding the complexes to the cells, the siRNA and Lipofectamine 2000 were diluted in Opti-MEM® I Reduced Serum Medium (Gibco, Grand Island, NY, USA) and combined. After incubation for 4–6 h, the transfection mixture was swapped out for fresh DMEM with 10% FBS. Cells were then let to develop for 48–72 h before

being subjected to additional examination. The effects of the siRNA therapy were evaluated and NRAS downregulation confirmed by quantitative PCR assays, which also validated transfection efficiency and gene silencing.

2.7 Cell viability and clonogenic survival assay

A 96-well plate was used to evenly distribute SK-Hep-1 and HUH7 cells, with 3×10^3 cells per well. For 48 h following seeding, the cells were exposed to either ML-323 or 0.1% DMSO. Following the instructions provided by the manufacturer, the Cell Counting Pack 8 (CCK-8, Beyotime Biotechnology, Nantong, China) was used to choose the cell attainability. When 10 µL of CCK-8 reagent was applied to each well and incubated for one to two hours at 37 °C, the absorbance at 450 nm was measured using a microplate reader. Cell viability percentages can be calculated using the absorbance readings, which correlate with the amount of viable cells. In duplicate, for the colony formation experiment, 500 cells were seeded into individual wells of a 6-well plate. After being cultured for 10 days, the cells were treated with DMSO or ML-323. To keep the development conditions ideal, the medium was changed every three to four days during this time. After a 10-day incubation period, the colonies were subjected to a 15-min incubation at room temperature in the presence of 4% paraformaldehyde. Crystal violet was used to dye the cells for 20 min after fixation in order to reveal the colonies. The colonies were counted under a light microscope after the excess dye was rinsed off with distilled water. Colony count is a good indicator of cell proliferation and survival in response to various therapies.

2.8 RNA extraction and determination

Cellular RNA was isolated by following the manufacturer's procedure for the TRIzol reagent, which was purchased from Shanghai Harin Biotechnology Co., Ltd. Cells were first lysed in TRIzol, and then chloroform phase separation was used to separate the RNA from the DNA and protein. After that, isopropanol was used to precipitate the RNA, followed by ethanol washing and subsequent dissolution in RNase-free water. Spectrophotometers or nano-drop devices were used to measure the concentration and purity of the RNA that was extracted. Takara Biotechnology Co., Ltd. of Dalian, China, provided the reverse transcription kit that was used to create cDNA from the total RNA. The reaction was conducted at particular temperatures to generate complementary DNA by incubating RNA with reverse transcriptase, primers, and deoxyribonucleotides (dNTPs). Takara Biotechnology Co., Ltd. of Dalian, China, supplied the SYBR Premix Ex TaqTM II kit, which was used for quantitative real-time PCR (qRT-PCR). A real-time PCR apparatus was used to conduct the qRT-PCR reactions in a 96-well plate. A final volume of water, the forward and reverse primers, along with the SYBR Premix Ex TaqTM II master mix, were utilized in the experimental procedure., and cDNA sample were all components of each reaction. Denaturation was the first stage in the PCR process, Subsequently, a total of 40 amplification cycles were conducted. (denaturation, annealing, and extension). To ensure the PCR products were specific, a melting curve analysis was performed at the end. To ensure that the target genes' expression levels were normalized, GAPDH was utilized as an internal reference gene. In the $2^{-\Delta\Delta Ct}$ method, relative gene expression was determined by comparing the target gene's and reference gene's threshold cycle (Ct) values within each sample (ΔCt) and the experimental and control groups (ΔΔCt). RT-PCR for NRAS was carried out with the forward primer 5′- ATGACTGAGTACAAACTGGTGGT-3′ and reverse primer 5′- CATGTATTGGTC TCTCATGGCAC-3′. GAPDH forward: 5′- CTGGGCTACACTGAGCACC-3′ and reverse: 5′- AAGTGGTCGTTGAGGGCAATG-3′.

2.9 Statistical analysis

The data is shown as the average plus or minus the standard deviation (SD) in order to show how the data set is variable. With the help of GraphPad Prism 7.0, Created by GraphPad Software and situated in San Diego, California, United States of America., statistical analyses were carried out. In studies with more than one group, one-way analysis of variance (ANOVA) was used to compare the differences between them. After ANOVA found statistically significant differences, the specific groups that differed from each other were identified using the Least Significant Difference (LSD) post hoc test. When two groups were compared, the significance of the means was determined using Student's t-test. Assumptions of normality of distribution and equality of variances among the compared groups are fundamental to both parametric tests. A p-value below 0.05 ($p < 0.05$) was deemed to indicate statistical significance. At this level, we can say with confidence that the differences we've seen are statistically significant and not just coincidental. To make sure the results could be repeated and were reliable, every experiment was done three times. The results were double-checked by conducting each replicate on its own.

3 Results

3.1 Identification of differentially expressed NKCRGs involved prognosis in HCC patients in the TCGA Cohort

Firstly, we analyzed TCGA datasets(134 NKCRGs) by the use of "limma" packages and identified 24 differentially expressed NKCRGs in HCC specimens, including 22 upregulated genes(NRAS, HLA-G, CSF2, PAK1, PIK3R3, MAP2K2, TNFRSF10C, MAPK3, MICA, PRKCA, LAT, SHC1, HRAS, RAC3, PLCG1, MICB, PIK3R2, NFATC4, ULBP2, PRKCG, SHC3 and ULBP1) and 2 down-regulated genes(CD244 and KIR2DL1)(Fig. 1A). Then, we performed functional enrichment analysis. The results of GO analysis revealed that 24 differentially expressed NKCRGs were mainly enriched in the regulation of response to biotic stimulus, the pathway involving cell surface receptors that activate the immune response, signal transduction for immune response activation, and interactions occurring on the outer surface of the plasma membrane.cell – cell junction, anchored component of membrane, the interaction with phosphotyrosine residues, amino acids phosphorylated in proteins, and phosphoproteins binding were observed in the experimental results depicted in Fig. 1B. The results of KEGG analysis revealed that 24 differentially expressed NKCRGs were mainly associated with Natural killer cell-mediated cytotoxicity, ErbB signaling pathway, Glioma, VEGF signaling pathway, Fc epsilon RI signaling pathway, T cell receptor signaling pathway, Focal adhesion and Pathways in cancer (Fig. 1C). The results of DO analysis suggested that 24 differentially expressed NKCRGs were mainly associated with musculoskeletal system cancer, osteosarcoma, bone cancer, connective tissue cancer, autonomic nervous system neoplasm and neuroblastoma (Fig. 1D). Then, we performed Univariate analysis and identified 21 prognostic NKCRGs in HCC (Fig. 1E). In addition, the results of Venn Diagram confirmed eight differentially expressed NKCRGs involved prognosis in HCC, including PAK1, MAP2K2, MAPK3, PLCG1, SHC1, HRAS, NRAS and MICB (Fig. 1F and G). The association among these genetic factors was illustrated in Fig. 1H.

3.2 Construction of a prognostic model in the TCGA cohort and validation in in the ICGC cohort

To develop a predictive model, our group analyzed the expressions of the specified four genes using the LASSO-Cox regression methodology. LASSO-Cox regression is a statistical method that combines LASSO regression and the Cox proportional hazards model, commonly used in survival analysis in biostatistics and medical research. The ideal value of γ was used to determine a marker for four genes (Figs. 2A and B). This is how the risk score came to be: The expressions of MAP2K2, SHC1, HRAS, and NRAS were multiplied by 0.110, 0.215, 0.255, and 0.463, respectively, to get the score. Based on the median threshold value, patients were categorized into two groups. Overall survival (OS) was considerably lower in the high-risk group compared to the low-risk group, according to the Kaplan–Meier curve (Fig. 2C, $P < 0.001$). The data presented in Fig. 2D indicated that the prognostic model achieved an AUC of 0.738 for survival prediction within a one-year timeframe. the values of 0.692 at the end of 2 years and 0.662 at the end of 3 years were obtained from time-dependent ROC curves. Patients from ICGA datasets were stratified into high-risk or low-risk categories using the median value derived from the TCGA cohort. This approach was employed to evaluate the robustness of the model developed from the TCGA cohort. Compared to the low-risk group, the high-risk group's patients had a lower survival time (Fig. 2E). Figure 2F illustrated that the 4-gene signature exhibited an area under the curve (AUC) of 0.756 at the end of 1 year, 0.724 at the end of 2 years, and 0.701 at the end of 3 years. Both the TCGA (Fig. 2G) and the ICGC (Fig. 2H) datasets demonstrated, Through the application of PCA and t-SNE techniques, it was observed that individuals belonging to distinct risk categories exhibited varied spatial distributions. To find out if the risk score was a factor that predicted OS on its own, researchers used univariate and multivariate Cox analyses. Figures 2I and J showed that in univariate Cox analysis, there was a substantial correlation between OS and risk scores in both the TCGA and ICGC cohorts. In both the TCGA and ICGC cohorts, multivariate Cox analysis confirmed that the risk score remained a significant independent predictor of overall survival (OS), as depicted in Figs. 2I and J, even when accounting for other potential confounding variables.

3.3 Prognostic model risk score and clinical features

By examining the correlation between the risk score and clinical attributes of patients diagnosed with HCC, we investigated its relationship with gender, age, tumor grade, and tumor stage. Statistical analyses, including t-tests for gender and correlation analysis for age, revealed that the risk score was not significantly associated with either gender or age in the TCGA dataset (Figs. 3A and B). This indicates that the risk score is consistent across different

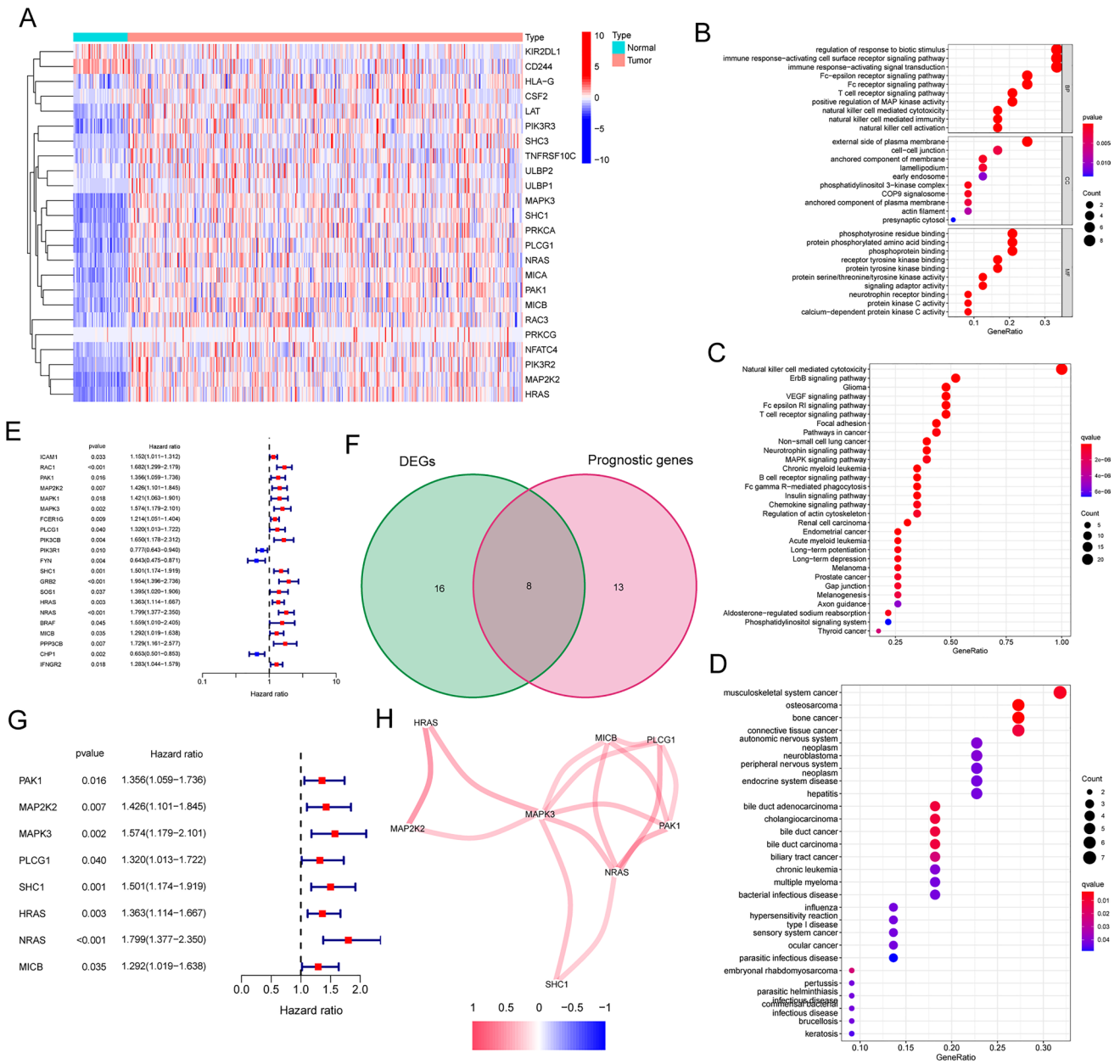

Fig. 1 Differentially Expressed NKCRGs and Their Functional Enrichment in HCC. **A** Identification of 24 differentially expressed NKCRGs in HCC specimens from the TCGA cohort. The figure shows 22 upregulated genes (NRAS, HLA-G, CSF2, PAK1, PIK3R3, MAP2K2, TNFRSF10C, MAPK3, MICA, PRKCA, LAT, SHC1, HRAS, RAC3, PLCG1, MICB, PIK3R2, NFATC4, ULBP2, PRKCG, SHC3, and ULBP1) and 2 downregulated genes (CD244 and KIR2DL1). **B** GO analysis results for the 24 differentially expressed NKCRGs. **C** KEGG pathway analysis showing associations of the 24 differentially expressed NKCRGs with pathways including Natural killer cell mediated cytotoxicity, ErbB signaling pathway, Glioma, and VEGF signaling pathway. **D** Disease Ontology (DO) analysis indicating associations of the 24 differentially expressed NKCRGs with musculoskeletal system cancer, osteosarcoma, bone cancer, and neuroblastoma. **E** Univariate analysis results identifying 21 prognostic NKCRGs in HCC. **F**, **G** Venn diagram identifying eight differentially expressed NKCRGs involved in prognosis in HCC: PAK1, MAP2K2, MAPK3, PLCG1, SHC1, HRAS, NRAS, and MICB. (H) Correlation analysis showing relationships between the eight prognostic NKCRGs

genders and age groups. In contrast, the risk score was significantly higher in patients with advanced tumor grades and stages, as determined by ANOVA or Kruskal–Wallis tests (Fig. 3C and D). This indicates that elevated risk scores are correlated with more pronounced tumor attributes., reflecting tumor progression. To validate these findings, we conducted similar analyses on the ICGC dataset, it was verified that patients with advanced tumor stages consistently exhibited elevated risk scores. (Fig. 3E–G). These findings highlight the significance of the risk assessment score in predicting potential outcomes. as a reliable indicator of tumor severity and highlight its clinical relevance

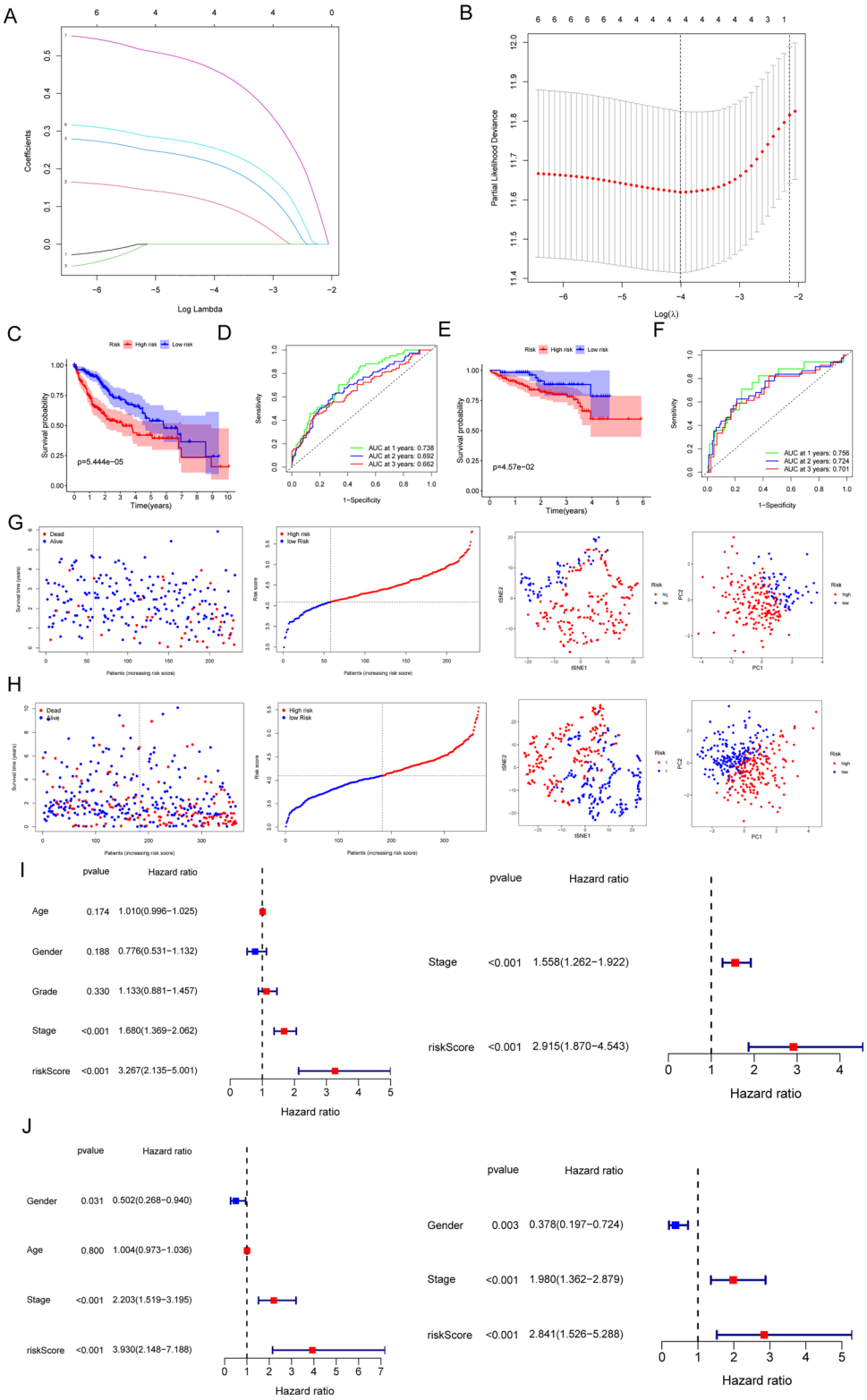

Fig. 2 Building and Testing a Prognostic Model. **A**, **B** By analyzing the expression profiles of four genes, LASSO-Cox regression analysis was used to get the best values for the prognostic model. **C** The prognostic model in the TCGA cohort revealed variations in overall survival between the low-risk and high-risk groups, as shown by the Kaplan–Meier survival curves ($P < 0.001$). **D** The prognostic model's time-dependent ROC curves show 3 year AUC values of 0.662, 2 year AUC values of 0.692, and 1 year AUC values of 0.738. **E** Kaplan–Meier survival curves for the ICGC cohort, showing that the prognostic model is accurate with equivalent results for low-risk and high-risk survival. **F** The 4-gene signature's time-dependent ROC curves in the ICGC cohort. **G**, **H** Statistical analysis using PCA and t-SNE reveals that the ICGC and TCGA cohorts have different distributions of patients at high and low risk. I and J are the Cox analyses for univariate and multivariate data

in stratifying patients based on tumor progression rather than demographic factors. Future research could further explore the biological mechanisms linking the risk score to tumor progression and assess its predictive value in combination with other biomarkers.

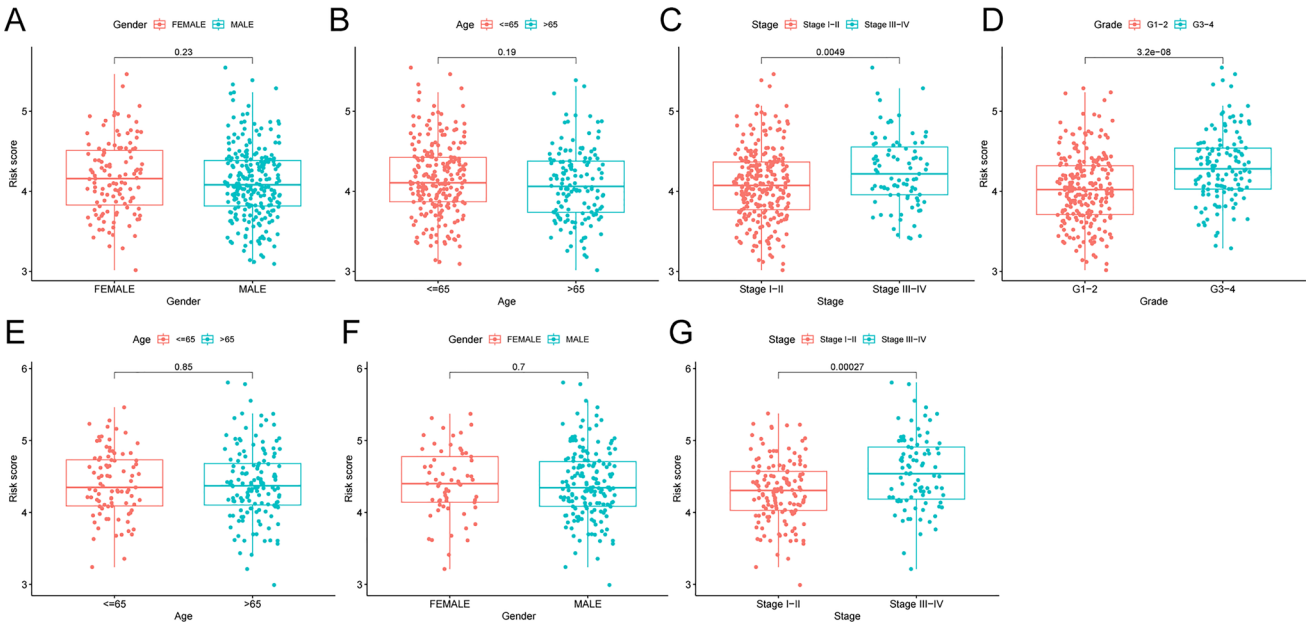

Fig. 3 Association of Risk Score with Clinical Features. **A**, **B** Analysis of the association between risk score and clinical features such as gender and age in the TCGA cohort. No significant correlation with gender or age. **C**, **D** Higher risk scores associated with advanced tumor grades and stages in the TCGA cohort, as determined by ANOVA or Kruskal–Wallis tests. **E**–**G** Validation of the association between risk score and tumor stages in the ICGC dataset, confirming that higher risk scores correlate with advanced tumor stages

3.4 Analysis of immune status and the tumor microenvironment

SsGSEA (single-sample Gene Set Enrichment Analysis) is a gene set enrichment analysis method used to assess the activity or expression level of a gene set in an individual sample. Unlike the traditional GSEA (Gene Set Enrichment Analysis), which typically evaluates the enrichment of a gene set across a group of samples, ssGSEA extends the GSEA approach to each individual sample, allowing for the calculation of the enrichment score of a gene set within each sample. Using ssGSEA, we conducted a quantitative analysis to measure the enrichment scores of various subpopulations of immune cells, their associated functions, and pathways. This investigation aimed to further explore the connection between risk scores and the immunological status of the subjects. There was an increase in the proportion of aDCs, B cells, macrophages, mast cells, neutrophils, NK cells, Tfh, and Treg in the high-risk group when compared to the low-risk group (Fig. 4A and B). In addition, the group at elevated risk exhibited elevated scores in APC co-stimulation and MHC class I. whereas the inverse was true for Cytolytic_activity. Figures 4C and D showed that the ICGC cohort's comparisons between the two risk groups were comparable to the TCGA's. The results shown in Fig. 4E illustrate the outcomes of our investigation into immune infiltration within HCC using TCGA data and its association with the risk score. We found that C1 was substantially associated with high-risk score and C4 with low risk score. Two methods for quantifying tumor stemness include the DNAss, which is derived from DNA methylation patterns, and the RNAss, which is based on mRNA expression levels. When evaluating the tumor's immunological microenvironment, the stromal score and immune score were used. An investigation of the possible link between the risk score and tumor stem cells and the immune microenvironment was carried out using a correlation analysis. No statistically significant correlation was found between risk score and DNAss or RNAss, according to the results. Figures 4F-I showed that there was a positive connection ($P < 0.001$) between the risk score and the immunological score.

3.5 The expression of HRAS, SHC1, MAP2K2, NRAS and chemo-sensitivity of cancer cells

We examined correlations between medication sensitivity and the expressions of genes associated with prognosis in the NCI-60 cell line. Some genes related to prognosis were shown to be associated with sensitivity to certain chemotherapy treatments ($p < 0.01$). For example, Fig. 5 showed that cancer cells were more sensitive to Palbociclib,

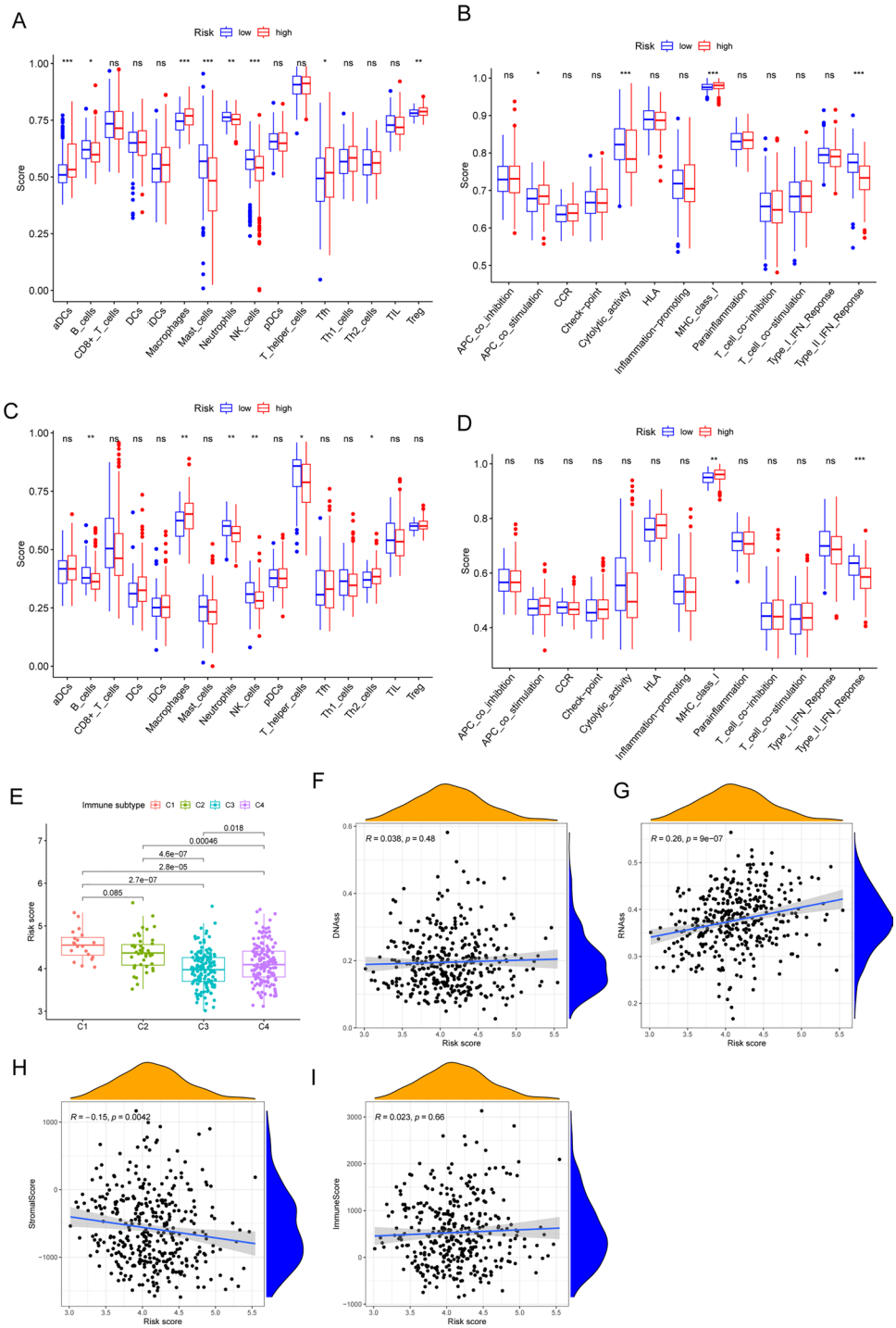

Fig. 4 Risk Score Correlation with Immune Status and Tumor Microenvironment. **A**, **B** Enrichment scores of immune cell subpopulations and related functions, showing higher fractions of aDCs, B_cells, Macrophages, Mast_cells, Neutrophils, NK_cells, Tfh, and Treg in the high-risk group. **C**, **D** Similar immune cell and function comparisons in the ICGC cohort, confirming findings from the TCGA dataset. **E** Correlation of risk score with immune subtypes, showing a significant association with C1 (wound healing) and C4 (lymphocyte depleted) immune subtypes. **F–I** Correlation analysis of risk score with tumor stemness (DNAss and RNAss) and immune score, indicating a significant positive correlation with immune score but not with DNAss or RNAss. Data are expressed as mean ± SD from triplicate experiments, with statistical significance indicated (*p < 0.05, **p < 0.01)

Irofulven, Bleomycin, Floxuridine, Irofulven, Simvastatin, Lenvatinib, Cladribine, Gemcitabine, and Floxuridine when their expression of HRAS, SHC1, MAP2K2, and NRAS was higher.

3.6 The expression pattern of HRAS, SHC1, MAP2K2, NRAS in HCC and their survival analysis

Then, we analyzed the expression pattern of HRAS, SHC1, MAP2K2, NRAS in HCC from TCGA datasets and found that their expressions were distinctly increased in HCC specimens compared with non-tumor specimens(Fig. 6A and B). Moreover, we performed K-M survival analysis and found that high expressions of HRAS, MAP2K2 and NRAS was associated a shorter

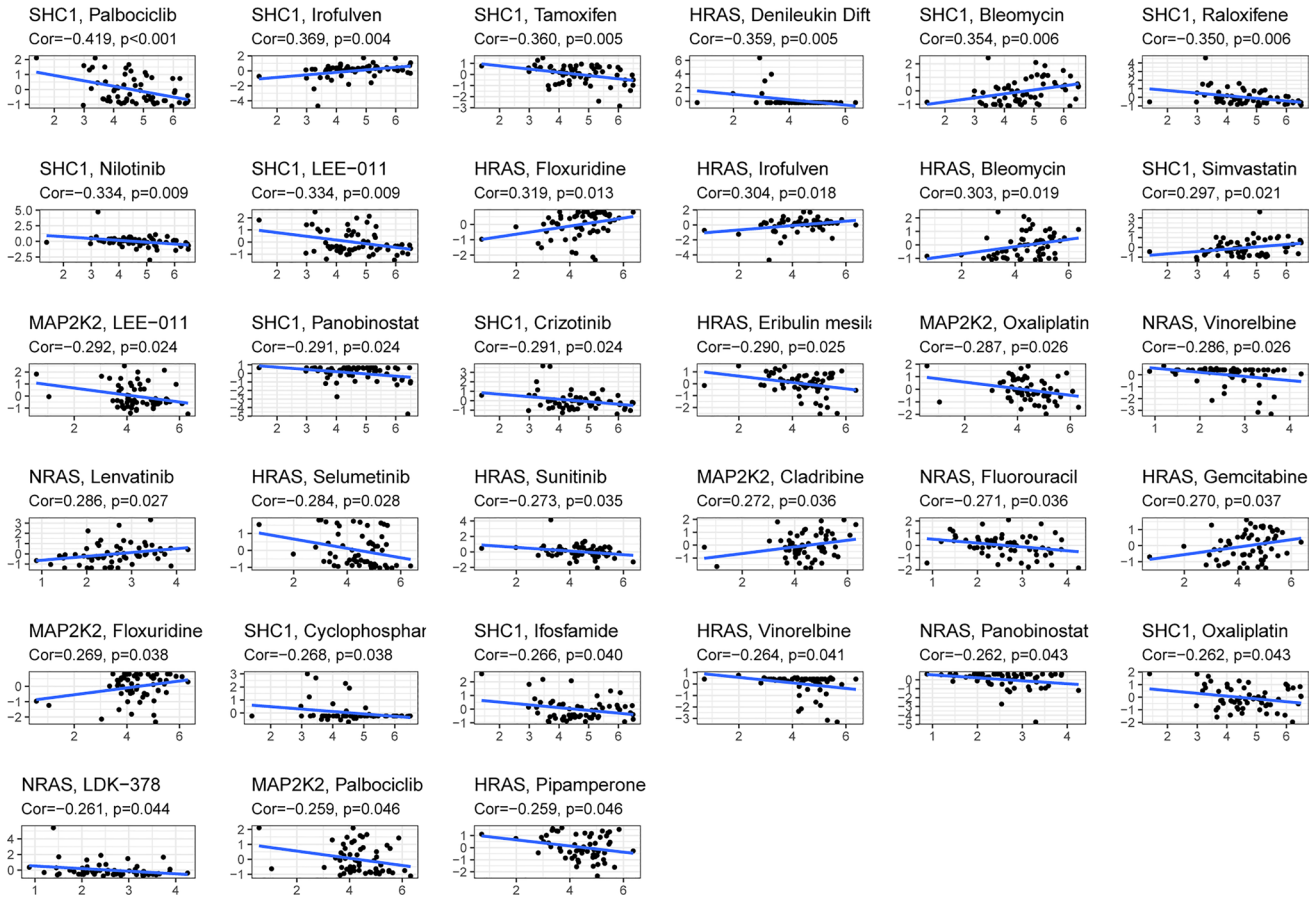

Fig. 5 Association of prognosis-related gene expression with drug sensitivity

overall survival in HCC patients, while SHC1 expression did not showed a distinct result(Fig. 6C). Moreover, we analyzed association between the expression of HRAS, SHC1, MAP2K2, NRAS, and progression-free survival. As shown in Fig. 6D, only HRAS and NRAS predicted a shorter progression-free survival in patients with high RAS and NRAS expression. In addition, the results of the Time-ROC assays were shown in Fig. 6E. Furthermore, It was noted that individuals exhibiting elevated levels of HRAS, SHC1, MAP2K2, and NRA exhibited an advanced stage and grade (Fig. 7A–D). Finally, our group carried out univariate and multivariate analysis and the results indicated that HRAS, SHC1, and NRAS were independent predictors for overall survival of HCC patients (Fig. 8A–D).

3.7 Knockdown of NRAS suppressed the proliferation of HCC cells

Among HRAS, SHC1, MAP2K2, and NRAS, our attention focused on NRAS because its function in HCC was rarely reported. Then, we performed RT-PCR and confirmed that compared to LO2 cells, the expression of NRAS was much higher in four HCC cells (Fig. 9A). The results of RT-PCR confirmed that si-NRAS successfully suppressed the expression of NRAS in both HUH7 and SK-Hep-1 cells (Fig. 9B). Moreover, the results of CCK-8 assays and clone formation assays indicated that knockdown of NRAS distinctly suppressed the proliferation of HUH7 and SK-Hep-1 cells (Fig. 9C and D).

4 Discussion

The prognosis for HCC patients is influenced by several factors, including tumor stage, liver function, and response to treatment [25, 26]. Prognostic assessment primarily relies on various indicators. The BCLC staging system categorizes HCC into early, intermediate, advanced, and terminal stages based on tumor size, number, liver function, and overall patient health [27, 28]. While comprehensive, it may oversimplify individual variations. The AJCC/TNM staging system provides

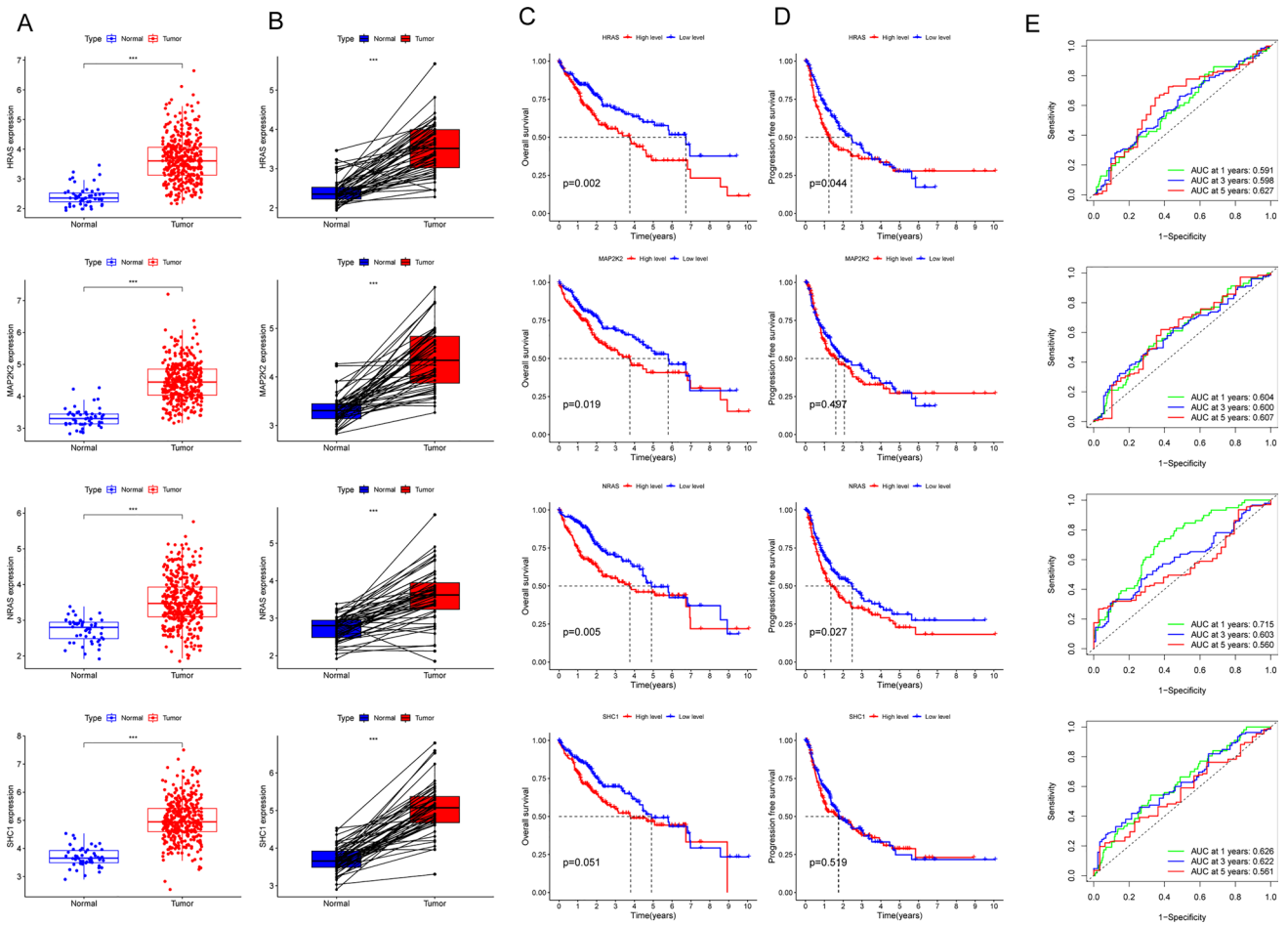

Fig. 6 Expression Patterns and Survival Analysis of HRAS, SHC1, MAP2K2, and NRAS. **A**, **B** Expression levels of HRAS, SHC1, MAP2K2, and NRAS in HCC compared to non-tumor specimens. **C** Kaplan–Meier survival analysis showing that high expression of HRAS, MAP2K2, and NRAS is associated with shorter overall survival in HCC patients. SHC1 expression did not show a significant result. **D** Association between expression levels of HRAS, SHC1, MAP2K2, and NRAS and progression-free survival, with HRAS and NRAS predicting shorter progression-free survival. **E** Time-ROC analysis demonstrating the predictive value of the expression levels of these genes. Data are expressed as mean ± SD from triplicate experiments, with statistical significance indicated (*$p < 0.05$, **$p < 0.01$)

detailed tumor, node, and metastasis information but may lack consideration of liver function and overall health [29, 30]. Liver function is evaluated using the Child–Pugh score, which assesses factors like bilirubin, albumin, and coagulation status, though it may not fully capture individual nuances [31, 32]. The MELD score, based on serum creatinine, bilirubin, and INR, is useful for liver transplant candidates but may not reflect tumor burden accurately. Biomarkers like alpha-fetoprotein (AFP) are commonly used for screening and monitoring but have limitations in sensitivity and specificity, particularly in early-stage or low-AFP tumors [33, 34]. Other biomarkers such as Glypican-3 and Des-gamma-carboxy prothrombin (DCP) offer additional insights but require further validation. Imaging techniques like CT, MRI, and ultrasound help determine tumor size and spread, yet they may not fully reflect liver function and tumor biology. Despite their utility, these prognostic methods have limitations and may benefit from integration with emerging biomarkers and novel assessment tools to enhance accuracy and tailor treatment strategies.

NK cells play a critical role in the immune system by identifying and eliminating infected or tumor cells. Their relationship with tumors, including HCC, is complex and multifaceted [35, 36]. NK cells are capable of recognizing and killing tumor cells by detecting abnormal surface markers or reduced MHC-I expression, which many tumors downregulate to evade immune surveillance [37]. They achieve this through the release of cytotoxic granules like perforin and granzymes, and by secreting cytokines such as interferon-γ and tumor necrosis factor-α to enhance immune responses. In the context of HCC, NK cell function can be impaired by the tumor microenvironment, which often includes factors that suppress NK cell activity, such as inhibitory cytokines or immune checkpoint molecules [38, 39]. Additionally, chronic inflammation and liver fibrosis associated with HCC may further affect NK cell function. Despite these challenges, NK

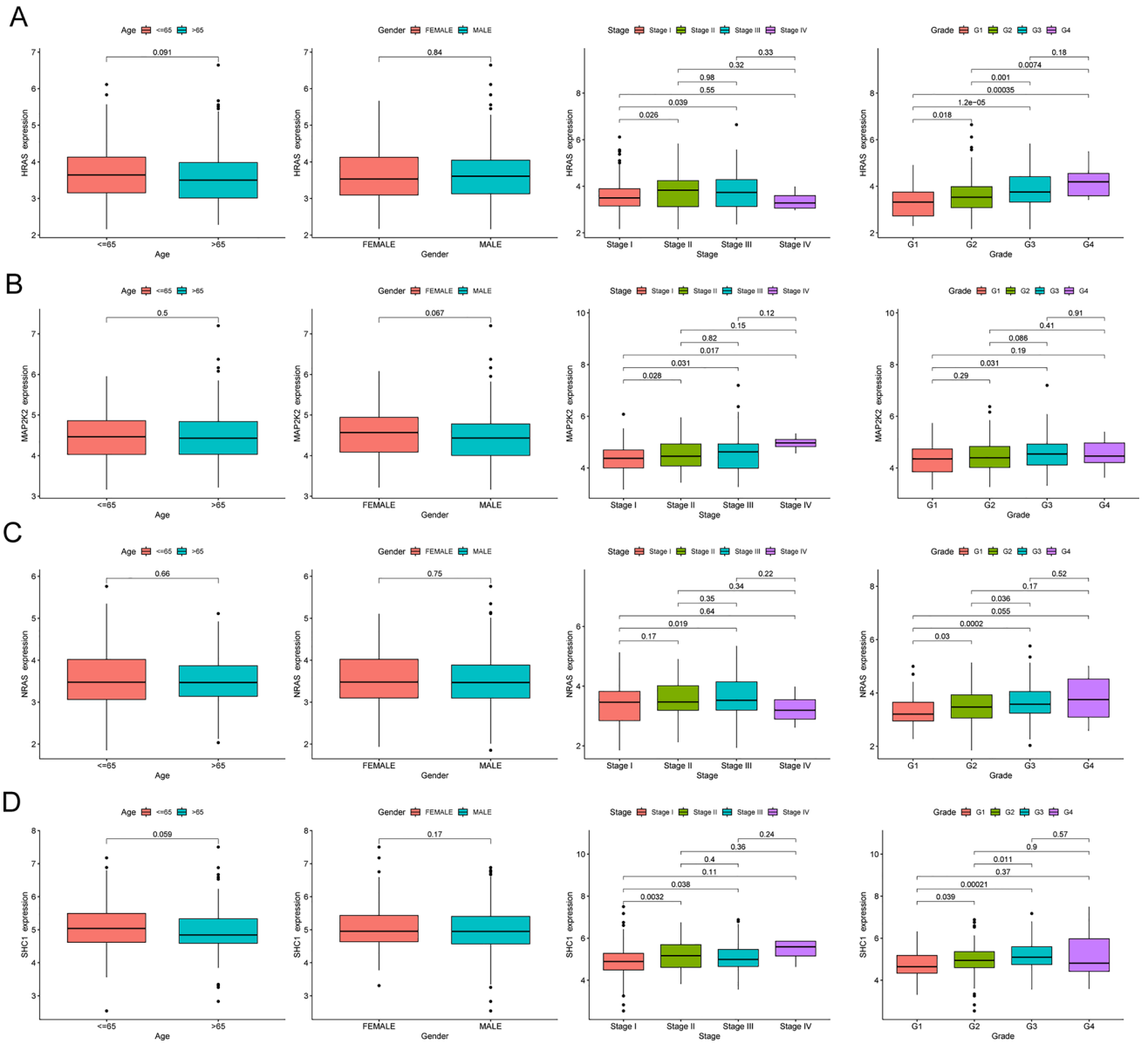

Fig. 7 Analysis of the expression levels of (**A**) HRAS, (**B**) MAP2K2, (**C**) NRAS and (**D**) SHC1 in relation to age, gender, tumor stage and grade

cell therapy presents a promising strategy for HCC treatment [40, 41]. By expanding and activating NK cells ex vivo and applying them to patients, the efficacy of existing treatments might be enhanced. However, the clinical application of NK cell therapy faces obstacles, including overcoming the suppressive tumor microenvironment and optimizing NK cell activation. However, we still don't know how NK cells work molecularly to fight tumors. So yet, there is no clinically-applicable, NK cell-based comprehensive assessment approach for TNBC prognosis and therapy efficacy prediction.

This study first identified 24 differentially expressed NK cell-related genes (NKCRGs) in HCC specimens from the TCGA dataset, including 22 upregulated and 2 downregulated genes. Functional enrichment analysis revealed that these genes were associated with biological stimulus response, immune activation pathways, and cancer-related pathways. Further univariate analysis identified 21 prognostic NKCRGs, and a Venn diagram confirmed that 8 key genes (PAK1, MAP2K2, MAPK3, PLCG1, SHC1, HRAS, NRAS, and MICB) were involved in HCC prognosis. A predictive model utilizing four pivotal genes (MAP2K2, SHC1, HRAS, NRAS) was constructed and validated in the ICGC dataset. The results showed that patients in the high-risk group had significantly worse overall survival compared to the low-risk group, with the model demonstrating good performance across different time points (AUC of 0.738 at 1 year, 0.692 at 2 years, and 0.662 at 3 years). PCA and t-SNE analyses indicated distinct distributions of patients in different risk groups within the datasets. Additionally,

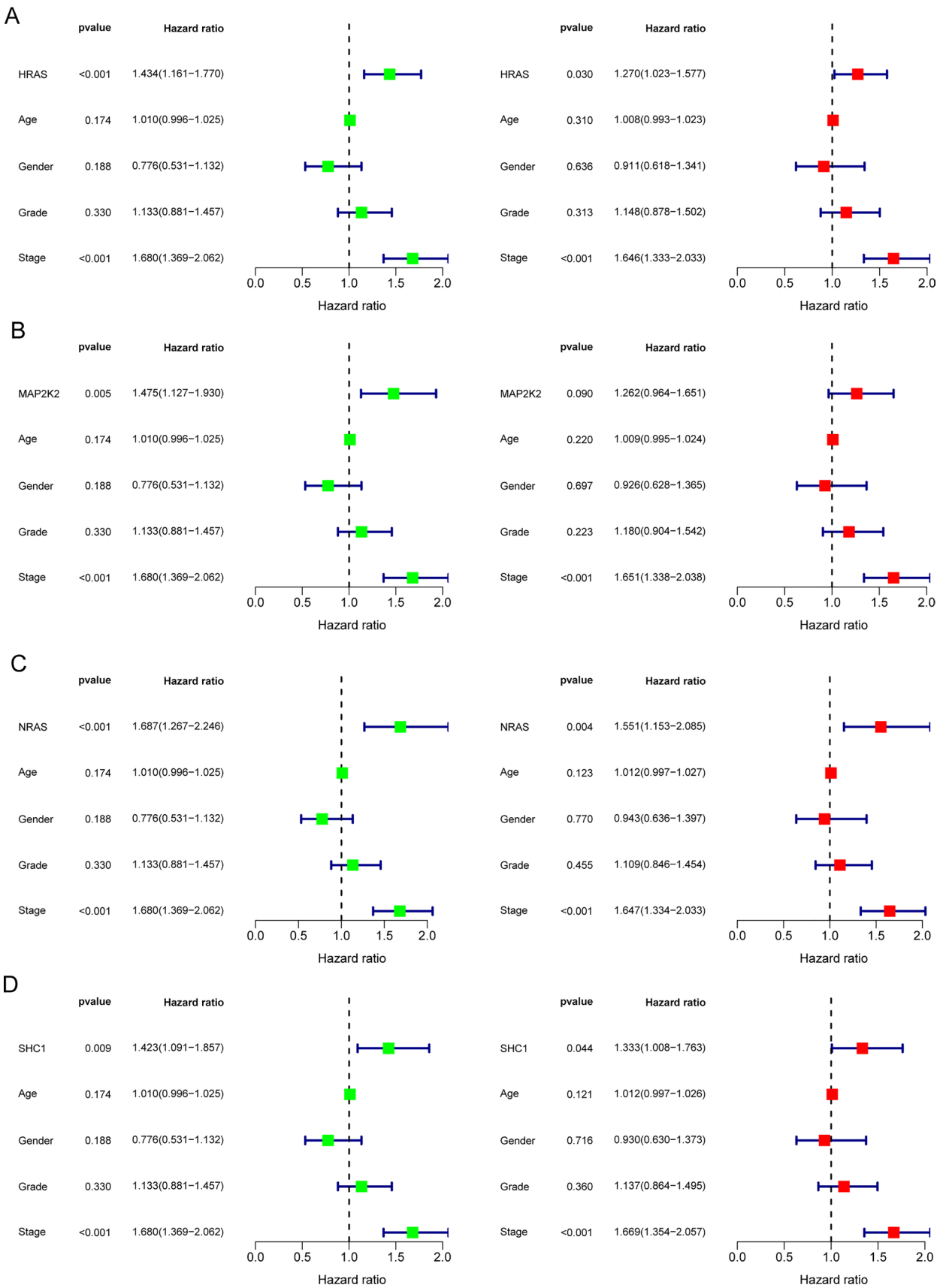

Fig. 8 Univariate and Multivariate Analysis of Independent Predictors including (**A**)HRAS, (**B**) MAP2K2, (**C**) NRAS and (**D**)SHC1 for Overall Survival

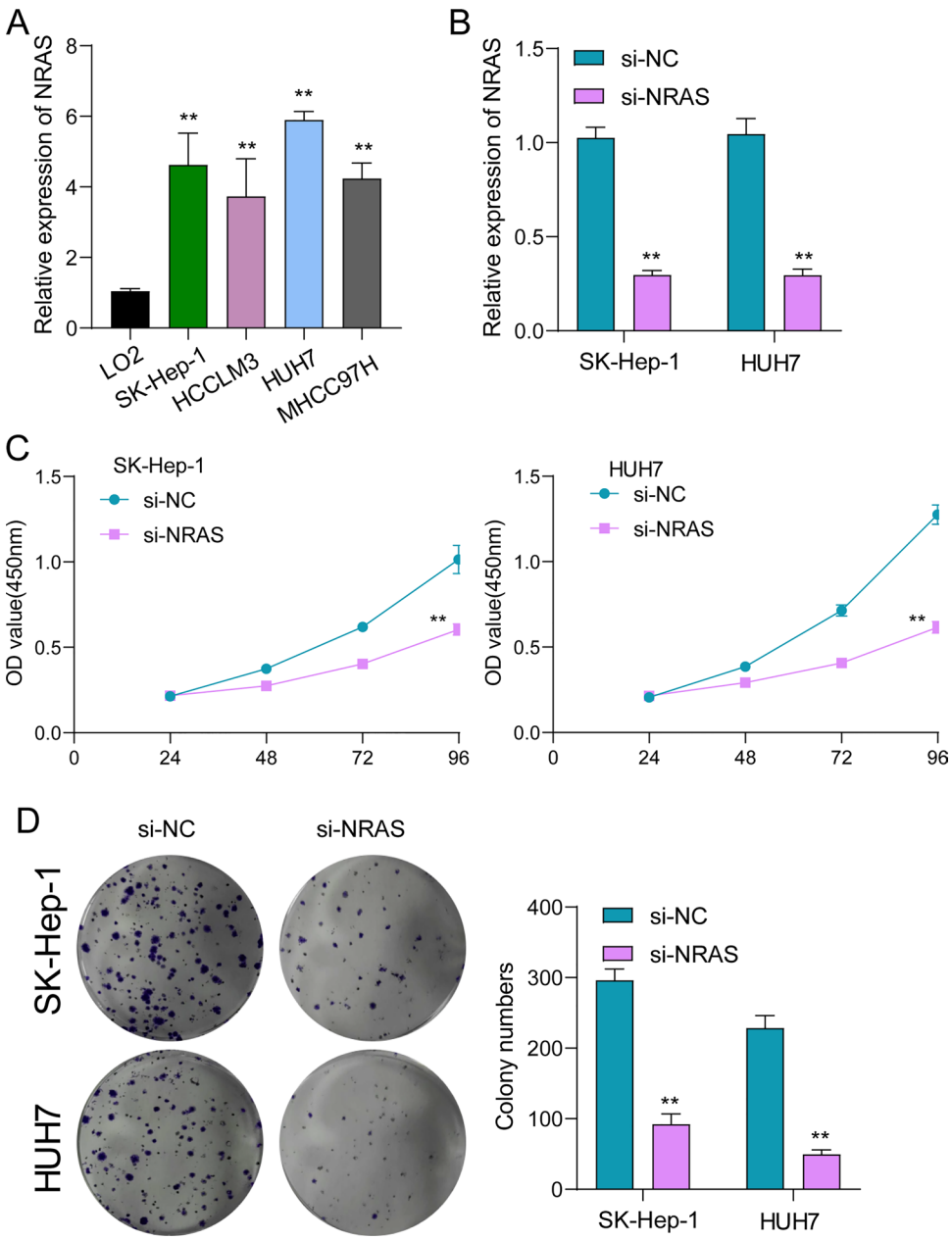

Fig. 9 Effects of NRAS Knockdown on HCC Cell Proliferation. **A** RT-PCR analysis confirming higher expression of NRAS in HCC cells compared to LO2 cells **B** RT-PCR results showing successful knockdown of NRAS in HUH7 and SK-Hep-1 cells. **C**, **D** CCK-8 and colony formation assays demonstrating that knockdown of NRAS significantly suppresses proliferation in HUH7 and SK-Hep-1 cells. Data are expressed as mean ± SD from triplicate experiments, with statistical significance indicated (*p < 0.05, **p < 0.01).

The risk assessment score demonstrated a statistically significant correlation with both the grade and stage of the tumor. but not with gender or age, suggesting that it is consistent across different demographic groups and correlates with more severe tumor characteristics. Validation within the ICGC dataset provided confirmation that the risk score serves as a dependable indicator of tumor stage.. These findings highlight the potential of the risk score as a valuable tool for assessing tumor severity in HCC patients and provide a basis for personalized treatment and further biomarker research.

Multiple noteworthy results emerged from the study's examination of immune state and tumor microenvironment in HCC [42]. In contrast to the low-risk group, the high-risk group showed elevated fractions of several immune cell types, such as regulatory T cells, activated dendritic cells, B cells, macrophages, mast cells, neutrophils, NK cells, and follicular helper T cells [43, 44]. It appears that high-risk tumors have an immune landscape that is more intricate. In the group at high risk, researchers found that MHC class I expression and APC co-stimulation were both elevated. while cytolytic activity was diminished, suggesting a possible decline in immune-mediated cancer cell apoptosis [45, 46]. The risk score was linked to the C1 immune subtype. (wound healing) in high-risk tumors and the C4 subtype (lymphocyte depleted) in low-risk tumors, reflecting a more pro-tumorigenic immune profile in high-risk cases. Additionally, there was no significant correlation between the risk score and the stemness scores based on DNA or RNA. it

was positively associated with immune scores, highlighting its relevance in assessing the immune microenvironment. The study also found that high expression of prognosis-related genes (HRAS, SHC1, MAP2K2, NRAS) was linked to increased sensitivity of cancer cells to various chemotherapy drugs, suggesting that these genes could be potential targets to enhance treatment efficacy. Overall, these findings emphasize the importance of integrating immune features into prognostic models and therapeutic strategies for more personalized treatment approaches in HCC.

NRAS is a member of the RAS family of small GTPases, playing a crucial role in regulating cell growth, differentiation, and survival [47, 48]. The protein encoded by the NRAS gene is pivotal in cell signaling, primarily through its role in activating downstream signaling pathways such as the RAF-MEK-ERK (MAPK) pathway and the PI3K-AKT pathway [49, 50]. These pathways are essential for cell proliferation and survival. Mutations in NRAS are commonly found in various malignancies, including melanoma, leukemia, and certain types of lymphomas [51–53]. In these cancers, NRAS mutations lead to constitutive activation of the NRAS protein, promoting uncontrolled proliferation and survival of cancer cells. Specifically, mutations in NRAS typically occur in its GTP-binding region, resulting in persistent activation and enhanced activity of downstream signaling pathways, thereby contributing to tumorigenesis. In recently, multiple research studies have indicated that NRAS plays a significant role in the advancement of various types of tumors. In HCC, NRAS mutations are relatively rare, but the role of NRAS in tumorigenesis and progression remains of interest. Studies suggest that overexpression or heightened activity of NRAS may be associated with the biological characteristics and prognosis of HCC [54, 55]. In this study, we also reported that NRAS was highly expressed in HCC specimens and associated with poor prognosis of HCC patients. In addition, we found that knockdown of NRAS distinctly suppressed the proliferation of HCC cells. Overall, these results highlight the potential of NRAS as a therapeutic target in HCC. Focusing on NRAS or the pathways it activates could be a way to stop the growth of tumors and enhance the prognosis for patients.

This study has several limitations. Firstly, although the study used TCGA and ICGC datasets for validation, the sample size may be relatively limited, especially for genes with low expression or rare subtypes of HCC. Additionally, the lack of independent laboratory validation and clinical validation may affect the reliability and generalizability of the model in clinical applications. Secondly, although this study suggests that genes such as NRAS may serve as therapeutic targets, there is a lack of clinical trials or in vitro and in vivo experimental validation for these genes. Further experimental research is needed to verify their potential role in HCC treatment and to ensure their feasibility and effectiveness as therapeutic targets.

5 Conclusion

Our study identified 24 differentially expressed NKCRGs in HCC, with eight genes significantly associated with prognosis. A LASSO-Cox regression model effectively categorized patients into high-risk and low-risk groups, demonstrating strong predictive power across TCGA and ICGC cohorts. High-risk scores were linked to advanced tumor stages and pro-tumor immune profiles. Elevated expression of HRAS, SHC1, MAP2K2, and NRAS in HCC tissues correlated with poorer survival. NRAS knockdown reduced cell proliferation, suggesting its potential as a therapeutic target. Future research should explore the mechanisms of these genes in HCC progression and validate them in clinical trials. Integrating additional biomarkers could enhance the model's accuracy and relevance for personalized treatment.

Acknowledgements Not applicable.

Author contributions Ruixi Li, Guangquan Zhang,Yingliang Li and Xianjie Shi developed a major research plan. Guangquan Zhang, Qiang Tao, Ziyun Wu, Xiaoping Liu, Rongrong Wang, Lei Liu and Yiran Niu perform experiments, analyze data, draw charts and write manuscripts. Kaile Du, Runpeng Wu, Fei Du, Xiyan Zheng and Yingliang Li helped collect data and references and provided technical support. All authors contributed to the article and approved the submitted version.

Funding This study was supported by Shenzhen Fundamental Research Program (JCYJ20220530144404010 & JCYJ20220530144404011) and Futian Healthcare Research Project No.FTWS2023037 and Futian District key specialty funding No. QZDZK-202413 and Outstanding Medical Innovation Talent Program of The Eighth Affiliated Hospital of Sun Yat-sen University No. YXYXCXRC202414 and Guangdong Foundation for Basic and Applied Research Enterprise Joint Fund No. 2023A1515220186 and Jiangxi Provincial Administration of Traditional Chinese Medicine Science and Technology Plan funding No.2024A0196.

Data availability The datasets generated during and/or analyzed during the current study are available from the corresponding author upon reasonable request.

Declarations

Ethics approval and consent to participate Not applicable.

Consent for publication Not applicable.

Competing interests The authors declare no competing interests.

References

1. Bray F, Laversanne M, Sung H, Ferlay J, Siegel RL, Soerjomataram I, Jemal A. Global cancer statistics 2022: GLOBOCAN estimates of incidence and mortality worldwide for 36 cancers in 185 countries. A Cancer J Clin. 2024;74(3):229–63.
2. Brown ZJ, Tsilimigras DI, Ruff SM, Mohseni A, Kamel IR, Cloyd JM, Pawlik TM. Management of hepatocellular carcinoma: a review. JAMA Surg. 2023;158(4):410–20.
3. Nagaraju GP, Dariya B, Kasa P, Peela S, El-Rayes BF. Epigenetics in hepatocellular carcinoma. Semin Cancer Biol. 2022;86(Pt 3):622–32.
4. Hartke J, Johnson M, Ghabril M. The diagnosis and treatment of hepatocellular carcinoma. Semin Diagn Pathol. 2017;34(2):153–9.
5. Renne SL, Sarcognato S, Sacchi D, Guido M, Roncalli M, Terracciano L, Di Tommaso L. Hepatocellular carcinoma: a clinical and pathological overview. Pathologica. 2021;113(3):203–17.
6. Kim E, Viatour P. Hepatocellular carcinoma: old friends and new tricks. Exp Mol Med. 2020;52(12):1898–907.
7. Chacko S, Samanta S. Hepatocellular carcinoma: a life-threatening disease. Biomed Pharmacother Biomed Pharmacother. 2016;84:1679–88.
8. Golabi P, Rhea L, Henry L, Younossi ZM. Hepatocellular carcinoma and non-alcoholic fatty liver disease. Hep Intl. 2019;13(6):688–94.
9. Xiao Y, Yu D. Tumor microenvironment as a therapeutic target in cancer. Pharmacol Ther. 2021;221: 107753.
10. Mehla K, Singh PK. Metabolic regulation of macrophage polarization in cancer. Trends in cancer. 2019;5(12):822–34.
11. Kalluri R, McAndrews KM. The role of extracellular vesicles in cancer. Cell. 2023;186(8):1610–26.
12. Nassar D, Blanpain C. Cancer stem cells: basic concepts and therapeutic implications. Annu Rev Pathol. 2016;11:47–76.
13. Dai E, Zhu Z, Wahed S, Qu Z, Storkus WJ, Guo ZS. Epigenetic modulation of antitumor immunity for improved cancer immunotherapy. Mol Cancer. 2021;20(1):171.
14. Heinhuis KM, Ros W, Kok M, Steeghs N, Beijnen JH, Schellens JHM. Enhancing antitumor response by combining immune checkpoint inhibitors with chemotherapy in solid tumors. Ann Oncol. 2019;30(2):219–35.
15. Toninelli M, Rossetti G, Pagani M. Charting the tumor microenvironment with spatial profiling technologies. Trends Cancer. 2023;9(12):1085–96.
16. Vivier E, Rebuffet L, Narni-Mancinelli E, Cornen S, Igarashi RY, Fantin VR. Natural killer cell therapies. Nature. 2024;626(8000):727–36.
17. Mimpen M, Smolders J, Hupperts R, Damoiseaux J. Natural killer cells in multiple sclerosis: a review. Immunol Lett. 2020;222:1–11.
18. Reid FSW, Egoroff N, Pockney PG, Smith SR. A systematic scoping review on natural killer cell function in colorectal cancer. Cancer Immunol Immunother. 2021;70(3):597–606.
19. Hodgins JJ, Khan ST, Park MM, Auer RC, Ardolino M. Killers 20: NK cell therapies at the forefront of cancer control. J Clin Investig. 2019;129(9):3499–510.
20. Tang J, Zhu Q, Li Z, Yang J, Lai Y. Natural killer cell-targeted immunotherapy for cancer. Curr Stem Cell Res Ther. 2022;17(6):513–26.
21. Ong S, Rose NR, Čiháková D. Natural killer cells in inflammatory heart disease. Clin Immunol. 2017;175:26–33.
22. Guo F, Zhang Y, Bai L, Cui J. Natural killer cell therapy targeting cancer stem cells: old wine in a new bottle. Cancer Lett. 2023;570: 216328.
23. Arellano-Ballestero H, Sabry M, Lowdell MW. A killer disarmed: natural killer cell impairment in myelodysplastic syndrome. Cells. 2023. https://doi.org/10.3390/cells12040633.
24. Gardiner CM. NK cell metabolism. J Leukoc Biol. 2019;105(6):1235–42.
25. Kim DW, Talati C, Kim R. Hepatocellular carcinoma (HCC): beyond sorafenib-chemotherapy. J Gastrointest Oncol. 2017;8(2):256–65.
26. El Jabbour T, Lagana SM, Lee H. Update on hepatocellular carcinoma: pathologists' review. World J Gastroenterol. 2019;25(14):1653–65.
27. Hall Z, Chiarugi D, Charidemou E, Leslie J, Scott E, Pellegrinet L, Allison M, Mocciaro G, Anstee QM, Evan GI, et al. Lipid remodeling in hepatocyte proliferation and hepatocellular carcinoma. Hepatol. 2021;73(3):1028–44.
28. Frau M, Feo F, Pascale RM. Pleiotropic effects of methionine adenosyltransferases deregulation as determinants of liver cancer progression and prognosis. J Hepatol. 2013;59(4):830–41.
29. Wang Y, Deng B. Hepatocellular carcinoma: molecular mechanism, targeted therapy, and biomarkers. Cancer Metastasis Rev. 2023;42(3):629–52.
30. Tayob N, Kanwal F, Alsarraj A, Hernaez R, El-Serag HB. The performance of AFP, AFP-3, DCP as biomarkers for detection of hepatocellular carcinoma (HCC): a phase 3 biomarker study in the United States. Clin Gastroenterol Hepatol. 2023;21(2):415-423.e414.

31. Singal AG, Tayob N, Mehta A, Marrero JA, El-Serag H, Jin Q. Saenz de Viteri C, Fobar A, Parikh ND: GALAD demonstrates high sensitivity for HCC surveillance in a cohort of patients with cirrhosis. Hepatology. 2022;75(3):541–9.
32. He Q, Yang J, Jin Y. Immune infiltration and clinical significance analyses of the coagulation-related genes in hepatocellular carcinoma. Brief Bioinform. 2022;23(4):2.
33. Xing X, Cai L, Ouyang J, Wang F, Li Z, Liu M, Wang Y, Zhou Y, Hu E, Huang C, et al. Proteomics-driven noninvasive screening of circulating serum protein panels for the early diagnosis of hepatocellular carcinoma. Nat Commun. 2023;14(1):8392.
34. Christou C, Stylianou A, Gkretsi V. Midkine (MDK) in hepatocellular carcinoma: more than a biomarker. Cells. 2024;13(2):136.
35. Becker PS, Suck G, Nowakowska P, Ullrich E, Seifried E, Bader P, Tonn T, Seidl C. Selection and expansion of natural killer cells for NK cell-based immunotherapy. Cancer Immunol Immunother. 2016;65(4):477–84.
36. Terrén I, Orrantia A, Vitallé J, Zenarruzabeitia O, Borrego F. NK cell metabolism and tumor microenvironment. Front Immunol. 2019;10:2278.
37. O'Brien KL, Finlay DK. Immunometabolism and natural killer cell responses. Nat Rev Immunol. 2019;19(5):282–90.
38. Minetto P, Guolo F, Pesce S, Greppi M, Obino V, Ferretti E, Sivori S, Genova C, Lemoli RM, Marcenaro E. Harnessing NK Cells for Cancer Treatment. Front Immunol. 2019;10:2836.
39. Portale F, Di Mitri D. NK cells in cancer: mechanisms of dysfunction and therapeutic potential. Int J Mol Sci. 2023. https://doi.org/10.3390/ijms24119521.
40. Michel T, Poli A, Cuapio A, Briquemont B, Iserentant G, Ollert M, Zimmer J. Human CD56bright NK cells: an update. J Immunol. 2016;196(7):2923–31.
41. Waldhauer I, Steinle A. NK cells and cancer immunosurveillance. Oncogene. 2008;27(45):5932–43.
42. Jin MZ, Jin WL. The updated landscape of tumor microenvironment and drug repurposing. Signal Transduct Target Ther. 2020;5(1):166.
43. Pan Y, Yu Y, Wang X, Zhang T. Tumor-associated macrophages in tumor immunity. Front Immunol. 2020;11: 583084.
44. Park EG, Pyo SJ, Cui Y, Yoon SH, Nam JW. Tumor immune microenvironment lncRNAs. Brief Bioinf. 2022;23(1):504.
45. Chhabra Y, Weeraratna AT. Fibroblasts in cancer: unity in heterogeneity. Cell. 2023;186(8):1580–609.
46. Zanotelli MR, Zhang J, Reinhart-King CA. Mechanoresponsive metabolism in cancer cell migration and metastasis. Cell Metab. 2021;33(7):1307–21.
47. Randic T, Kozar I, Margue C, Utikal J, Kreis S. NRAS mutant melanoma: towards better therapies. Cancer Treat Rev. 2021;99: 102238.
48. Moore AR, Rosenberg SC, McCormick F, Malek S. RAS-targeted therapies: is the undruggable drugged? Nat Rev Drug Discov. 2020;19(8):533–52.
49. Waters AM, Der CJ. KRAS the critical driver and therapeutic target for pancreatic cancer. Cold Spring Harbor Perspect Med. 2018. https://doi.org/10.1101/cshperspect.a031435.
50. Elbaz Younes I, Sokol L, Zhang L. Rosai-dorfman disease between proliferation and neoplasia. Cancers. 2022. https://doi.org/10.3390/cancers14215271.
51. Johnson DB, Puzanov I. Treatment of NRAS-mutant melanoma. Curr Treat Options Oncol. 2015;16(4):15.
52. Chang E, Demirci H, Demirci FY. Genetic aspects of conjunctival melanoma: a review. Genes. 2023. https://doi.org/10.3390/genes14091668.
53. Gobitti C, Sindoni A, Bampo C, Baresic T, Giorda G, Alessandrini L, Canzonieri V, Franchin G, Borsatti E. Malignant struma ovarii harboring a unique NRAS mutation: case report and review of the literature. Hormones. 2017;16(3):322–7.
54. Song W, Zheng C, Liu M, Xu Y, Qian Y, Zhang Z, Su H, Li X, Wu H, Gong P, et al. TRERNA1 upregulation mediated by HBx promotes sorafenib resistance and cell proliferation in HCC via targeting NRAS by sponging miR-22-3p. Mol Ther. 2021;29(8):2601–16.
55. Klemm S, Evert K, Utpatel K, Muggli A, Simile MM, Chen X, Evert M, Calvisi DF, Scheiter A. Identification of DUSP4/6 overexpression as a potential rheostat to NRAS-induced hepatocarcinogenesis. BMC Cancer. 2023;23(1):1086.